the plant journal

SEB Society for Experimental Biology

The Plant Journal (2012) doi: 10.1111/j.1365-313X.2012.05044.x

Arabidopsis *VILLIN2* and *VILLIN3* act redundantly in sclerenchyma development via bundling of actin filaments

Chanchan Bao[1,2,†], Juan Wang[1,†], Ruihui Zhang[1,2], Baocai Zhang[3], Hua Zhang[1,2], Yihua Zhou[3] and Shanjin Huang[1,*]

[1]*Key Laboratory of Plant Molecular Physiology, Institute of Botany, Chinese Academy of Sciences, Beijing 100093, China,*

[2]*Graduate School of Chinese Academy of Sciences, Beijing 100049, China, and*

[3]*State Key Laboratory of Plant Genomics and National Center for Plant Gene Research, Institute of Genetics and Developmental Biology, Chinese Academy of Sciences, Beijing 100101, China*

Received 14 February 2012; revised 28 April 2012; accepted 1 May 2012.

*For correspondence (email sjhuang@ibcas.ac.cn).

†These authors contributed equally to this work.

SUMMARY

The organization of the actin cytoskeleton has been implicated in sclerenchyma development. However, the molecular mechanisms linking the actin cytoskeleton to this process remain poorly understood. In particular, there have been no studies showing that direct genetic manipulation of the actin cytoskeleton affects sclerenchyma development. Villins belong to the villin/gelsolin/fragmin superfamily and are versatile actin-modifying proteins. Several recent studies have implicated villins in tip growth of single cells, but how villins act in multicellular plant development remains largely unknown. Here, we found that two closely related villin isovariants from Arabidopsis, VLN2 and VLN3, act redundantly in sclerenchyma development. Detailed analysis of cross-sections from inflorescence stems of *vln2 vln3* double mutant plants revealed a reduction in stem size and in the number of vascular bundles; however, no defects in synthesis of the secondary cell wall were detected. Surprisingly, the *vln2 vln3* double mutation did not affect cell elongation of inter-fascicular fibers. Biochemical analyses showed that recombinant VLN2 was able to cap, sever and bundle actin filaments, similar to VLN3. Consistent with these biochemical activities, loss of function of *VLN2* and *VLN3* resulted in a decrease in the amount of F-actin and actin bundles in plant cells. Collectively, our findings demonstrate that VLN2 and VLN3 act redundantly in sclerenchyma development via bundling of actin filaments.

Keywords: actin dynamics, actin-binding protein, villin, sclerenchyma development, *Arabidopsis thaliana*

INTRODUCTION

Sclerenchyma tissues provide critical mechanical support for plant stems as well as a pathway for the transport of water, nutrients and signaling molecules. Proper development and maturation of sclerenchyma tissues are important for plant form and function. However, how the development of sclerenchyma tissues is regulated remains largely unknown. The actin cytoskeleton has been shown to arrange longitudinally during tracheary element differentiation (Chaffey *et al.*, 2000; Gardiner *et al.*, 2003), and several Arabidopsis mutants with defects in sclerenchyma development were shown to have disorganized actin cables (Hu *et al.*, 2003; Zhong *et al.*, 2004, 2005a), implying an indispensable role for the actin cytoskeleton during sclerenchyma development (Turner *et al.*, 2007). During sclerenchyma formation, actin filaments may be involved in cell division, cell expansion, deposition of the cell wall, or all of the above. However, the molecular mechanisms by which the actin cytoskeleton acts upon these processes remain poorly understood. To date, there have been no studies showing that direct genetic manipulation of the actin cytoskeleton affects the development of sclerenchyma.

Studies from mammalian, yeast and plant systems show that the organization and function of the actin cytoskeleton are regulated by a multitude of actin-binding proteins (ABPs) (Staiger and Blanchoin, 2006; Pollard and Cooper, 2009; Staiger *et al.*, 2010). Among these, villin, originally identified from the core actin bundles of intestinal epithelial cell microvilli (Bretscher and Weber, 1979; Matsudaira and Burgess, 1979), is a versatile actin-modifying molecule that nucleates actin assembly, caps the barbed end of actin filaments, bundles pre-existing actin filaments and severs actin filaments in a calcium-dependent fashion (Walsh *et al.*,

1984; Friederich *et al.*, 1989, 1990; McGough *et al.*, 2003; Silacci *et al.*, 2004; Su *et al.*, 2007; Khurana and George, 2008). However, there are several notable exceptions among this protein family. For example, VLN1 from Arabidopsis (Huang *et al.*, 2005) and Quail from *Drosophila* (Matova *et al.*, 1999) are simple actin bundlers, lacking the filament-capping and severing activities. This emphasizes the importance of examining biochemical activities for any uncharacterized villin isovariant. Loss of function of villin in mice does not affect the development of intestinal microvilli, but does cause defects in calcium-induced destruction of brush borders (Ferrary *et al.*, 1999). Mutations in the *Drosophila Quail* gene cause defects in actin bundle formation during oogenesis, and consequently induce female sterility (Mahajan-Miklos and Cooley, 1994; Matova *et al.*, 1999).

Plant villin homologs were initially identified from pollen of lily (*Lilium longiflorum*) by biochemical means (Nakayasu *et al.*, 1998; Yokota and Shimmen, 1998; Yokota *et al.*, 2003). One lily villin isovariant, 135-ABP, was shown to bundle actin filaments in a Ca^{2+}/calmodulin-dependent manner (Yokota *et al.*, 2000). Subsequent studies showed that 135-ABP nucleates actin assembly and caps the barbed end of actin filaments in a Ca^{2+}/calmodulin-independent manner (Yokota *et al.*, 2005). Recently, Arabidopsis VLN5 was also shown to bundle actin filaments in a Ca^{2+}/calmodulin-dependent manner (Zhang *et al.*, 2010), implying that dependence on Ca^{2+}/calmodulin may be conserved among calcium-sensitive plant villins. Injection of a 135-ABP antibody resulted in actin filament bundles in the transvacuolar strands of root hairs that were thinner and fewer than normal, providing the initial *in vivo* evidence for a role of villin in actin bundle formation and stability (Tominaga *et al.*, 2000).

Five villin-like genes are encoded in the Arabidopsis genome (Klahre *et al.*, 2000; Huang *et al.*, 2005). Recent studies showed that VLN3, VLN4 and VLN5 contain the full suite of actin-modifying activities (Khurana *et al.*, 2010; Zhang *et al.*, 2010, 2011), whereas VLN1 is a simple filament-bundling protein that lacks severing ability (Huang *et al.*, 2005; Khurana *et al.*, 2010). Moreover, using a reconstitution assay and time-lapse total internal fluorescence reflection microscopy (TIRFM), Khurana *et al.* (2010) demonstrated that VLN1 and VLN3 have distinct and overlapping functions in formation and turnover of actin filament bundles. As multiple villin isovariants co-exist in different tissues and cells during plant development, as supported by the available expression data (Klahre *et al.*, 2000; Ma *et al.*, 2005; Hruz *et al.*, 2008), the interactions between villin isovariants need to be studied in detail. Recent genetic studies showed that VLN4 and VLN5 are required for the stabilization of actin filaments and polarized cell expansion during tip growth of root hairs and pollen tubes, respectively (Zhang *et al.*, 2010, 2011), and VLN2 and VLN3 act redundantly to regulate cell elongation and directional organ growth (Van der Honing *et al.*, 2012). However, how the villin family integrates the function of the actin cytoskeleton during complex plant developmental processes remains largely unknown.

In this study, we found that VLN2 and VLN3 act redundantly in sclerenchyma development, but have no obvious effect on inter-fascicular fiber cell elongation. Loss of function of *VLN2* and *VLN3* decrease actin filament bundling, and this was well supported by an *in vitro* biochemical analysis showing that VLN2 is similar to the well-characterized VLN3 isovariant (Khurana *et al.*, 2010) and has a full range of actin-binding activities, including filament bundling. Taken together, these results suggest that VLN2 and VLN3 act redundantly in sclerenchyma development via bundling of actin filaments.

RESULTS

Phylogram and expression pattern of VLN2

VLN2 is quite suitable to investigate the functional relationship between villins and plant development because it is widely expressed throughout vegetative tissues (Figure S1A) (https://www.genevestigator.com/gv/index.jsp; Klahre *et al.*, 2000; Zhang *et al.*, 2010). Phylogenetic analysis based on protein sequences showed that VLN2 groups with VLN3, which was previously designated as a group II villin (Khurana *et al.*, 2010). Additionally, we found that the *VLN2* and *VLN3* expression patterns overlapped considerably (Figure S1A); this was confirmed by RT-PCR analysis of several tissues, including stems, pedicels, roots and hypocotyls (Figure S1B). Collectively, these data imply that VLN2 and VLN3 may function coordinately during Arabidopsis development.

Mature plants of the *vln2 vln3* double mutant develop a pendent stem phenotype

To dissect the developmental functions of VLN2, we analyzed two T-DNA insertion lines designated *vln2-1* and *vln2-2* (Figure 1a). Although partial transcripts both downstream and upstream of the T-DNA insertion sites were identified, no full-length *VLN2* transcript was detected for either allele in homozygous *vln2-1* and *vln2-2* plants (Figure 1b). To dissect the biological functions of *VLN3*, we analyzed one T-DNA insertion line, designated *vln3* (Figure 1a). RT-PCR analysis showed that no full-length *VLN3* transcript was detected in *vln3* homozygous plants (Figure 1c); we therefore assume that it is a knockout allele. To examine whether and how VLN2 and VLN3 act coordinately during Arabidopsis development, we generated *vln2 vln3* double mutants by crossing either *vln2-1* or *vln2-2* with *vln3*. RT-PCR analysis showed that neither *VLN2* nor *VLN3* full-length transcripts were detectable in the two double mutants (Figure 1b,c).

Our initial observations showed that loss of function of either *VLN2* or *VLN3* had no gross effects on overall plant development (Figure 1d). However, loss of function of both

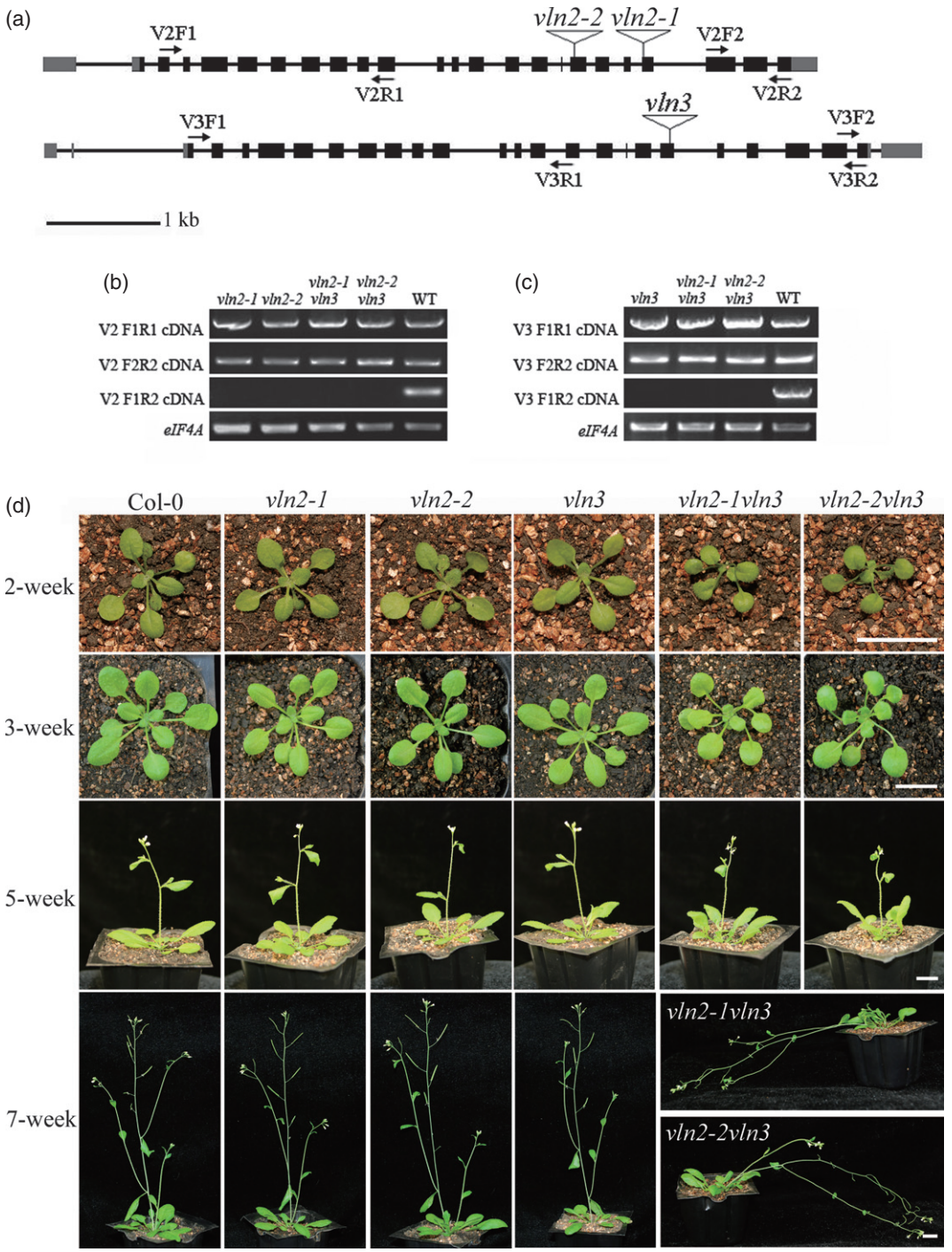

Figure 1. Loss of function of both *VLN2* and *VLN3* impairs the physical support of the plant.
(a) Physical structures of *VLN2* (At2g41740) and *VLN3* (At3g57410) genes. The untranslated regions, exons and introns are represented by gray boxes, black boxes and black lines, respectively. Both *VLN2* and *VLN3* have 23 exons and 22 introns. The T-DNA insertion lines are designated *vln2-1* (SAIL_613_C03) and *vln2-2* (SAIL_813_H02), with insertions in the 17th and 20th exons of *VLN2,* respectively, and *vln3* (SALK_078340) with an insertion in the 18th exon of *VLN3.*
(b, c) Three independent pairs of primers (F1/V2R1, F2/R2 and F1/R2; Table S2) were used to determine the level of *VLN2* and *VLN3* transcripts. The positions of primers are marked by arrows on *VLN2* and *VLN3* in (a).
(d) The inflorescence stems of *vln2 vln3* double mutants develop a pendent phenotype. The growth periods are indicated on the left, and the genotypes are indicated at the top. Scale bars = 1 cm.

VLN2 and *VLN3* caused developmental problems from the seedling stage to the mature plant stage (Figure 1d). At early stages, no major phenotypic differences were observed between *vln2 vln3* and Col-0 plants, but the *vln2 vln3* double mutants did have modestly twisted petioles and upward-growing rosette leaves (Figure 1d). At the mature

plant stage, the most obvious phenotype was that the *vln2 vln3* plants did not grow with an erect habit (Figure 1d). This pendent stem phenotype suggests that the mechanical strength necessary to support the plant is decreased in *vln2 vln3* plants. Indeed, the breaking force for the *vln2 vln3* stems was significantly less than that required for Col-0 stems (Figure 2). However, the force needed to pull *vln2* or *vln3* single mutant stems apart was not significantly different from that of Col-0 stems (Figure 2). Our complementation experiments showed that either *VLN2* or *VLN3* was sufficient to rescue the pendent stem phenotype of *vln2 vln3* double mutants (Figure S2). This, together with the data showing that the *vln2* or *vln3* single mutants did not show obvious phenotypes, suggests that *VLN2* and *VLN3* act redundantly to modulate inflorescence stem growth.

Loss of function of both *VLN2* and *VLN3* affects the development of sclerenchyma

We then cut thin cross-sections to investigate the anatomical defects of inflorescence stems. As shown in Figure 3, the width of inflorescence stems decreased significantly from 793 ± 18 μm for Col-0 (Figure 3a) to 608 ± 15 and 616 ± 14 μm for *vln2-1 vln3* and *vln2-2 vln3* plants, respectively (Figure 3d,g); however, there was no significant difference in the width of inflorescence stems of Col-0 compared to either *vln2* or *vln3* single mutants (Figures S3 and 3g). In addition, the number of vascular bundles decreased from 6.8 ± 0.3 for Col-0 to 5.2 ± 0.1 and 5.0 ± 0.1 for *vln2-1 vln3* and *vln2-2 vln3* plants, respectively (Figure 3h). Again, there was no significant difference in the number of vascular bundles between Col-0 and *vln2* or *vln3* single mutants (Figure S3 and Figure 3h). We also found that the region containing sclerenchyma cells, including inter-fascicular fibers and vascular bundles, was thinner in *vln2 vln3* stems (Figure 3e,f) compared to Col-0 stems (Figure 3b,c). The decrease in the number of sclerenchyma cell layers implied that differentiation or division of sclerenchyma cells was impaired. To compare the difference in sclerenchyma cells proportionally, we calculated the ratio whereby the cross-sectional area containing sclerenchyma cells was divided by the cross-sectional area of the entire inflorescence stem (Figure S4). Our results showed that the ratio decreased significantly from 31.3 ± 0.6% for Col-0 to 20.2 ± 0.8 and 20.0 ± 0.7% for *vln2-1 vln3* and *vln2-2 vln3* mutant plants, respectively (Figure 3i). We also carefully counted the cell number for different cell types in the inflorescence stem. The results showed that, although there was no difference in cell number in the epidermis when comparing *vln2 vln3* double mutants to Col-0 (Figure 3j), there was a significant reduction in the cell numbers in the cortex, inter-fascicular fibers, xylem and pith in *vln2 vln3* double mutants when compared to Col-0 (Figure 3j), implying that possible alteration of cell division may contribute to the defect of sclerenchyma development in *vln2 vln3* inflorescence stems. The defect in the development of the sclerenchyma was further confirmed by staining for lignin with phloroglucinol (Figure S5). The above results are consistent with the functions of sclerenchyma in providing physical support for plants. We also cut longitudinal sections of inflorescence stems and found that there was no obvious difference in the length of inter-fascicular fiber cells when Col-0 (462 ± 120 μm) was compared to *vln2-1 vln3*

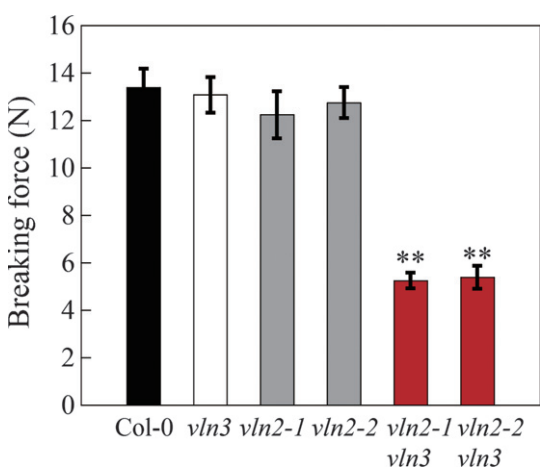

Figure 2. Less force is required to pull *vln2 vln3* inflorescence stems apart. The main stems of 7-week-old *Arabidopsis thaliana* plants of Col-0, *vln3*, *vln2-1*, *vln2-2*, *vln2-1 vln3* and *vln2-2 vln3* were measured. The maximum force required to break the stems was determined, and plotted as a function of each genotype. The measurement was repeated 12 times for each genotype. Values are means ± SE. $^{**}P < 0.01$ compared to Col-0 by Student's *t* test.

Figure 3. *VLN2* and *VLN3* act redundantly in the development of sclerenchyma.
(a–f) Cross-sections of vascular tissues from the basal portion of 7-week-old inflorescence stems of Col-0 and *vln2-1 vln3*.
(a) Cross-section of the basal portion of a stem from Col-0; (b) enlarged portion of (a) indicating the xylem region; (c) enlarged portion of (a) indicating the inter-fascicular fiber region.
(d) Cross-section of the basal portion of a stem from *vln2-1 vln3*; (e) enlarged portion of (d) indicating the xylem region; (f) enlarged portion of (d) indicating the inter-fascicular fiber region. ep, epidermis; co, cortex; en, endodermis; ph, phloem; xy, xylem; pi, pith; if, inter-fascicular fibers. Scale bars = 100 μm (a, d) and 50 μm (b, c, e, f).
(g) Quantification shows that the width of the stem decreased significantly in *vln2 vln3* double mutants. $^{**}P < 0.01$ compared to Col-0 by Student's *t*-test ($n = 10$).
(h) The number of vascular bundles decreased significantly in *vln2 vln3* double mutants. $^{**}P < 0.01$ compared to Col-0 by Student's *t*-test ($n = 10$).
(i) The development of sclerenchyma was impaired in *vln2 vln3* double mutants. For a definition of the ratio used to evaluate the development of sclerenchyma, see Figure S4. The ratio was plotted versus different genotypes. $^{*}P < 0.05$ and $^{**}P < 0.01$ compared to Col-0 by Student's *t*-test ($n = 10$).
(j) Quantification of cell number in inflorescence stems suggests that cell division may be affected in the stems of *vln2 vln3* double mutants. The numbers of cells in the epidermis, cortex, xylem, inter-fascicular fibers and pith of the stems were plotted. Values are means ± SD ($n = 10$). $^{*}P < 0.05$ and $^{**}P < 0.01$ compared to Col-0 by one-way ANOVA analysis.

(438 ± 94 μm) and *vln2-2 vln3* (429 ± 144 μm) (Figure S6). This implies that loss of function of both *VLN2* and *VLN3* did not affect inter-fascicular fiber cell elongation.

We next sought to determine whether loss of function of *VLN2* and *VLN3* affects the synthesis of secondary cell walls, which are the characteristic feature of sclerenchyma cells.

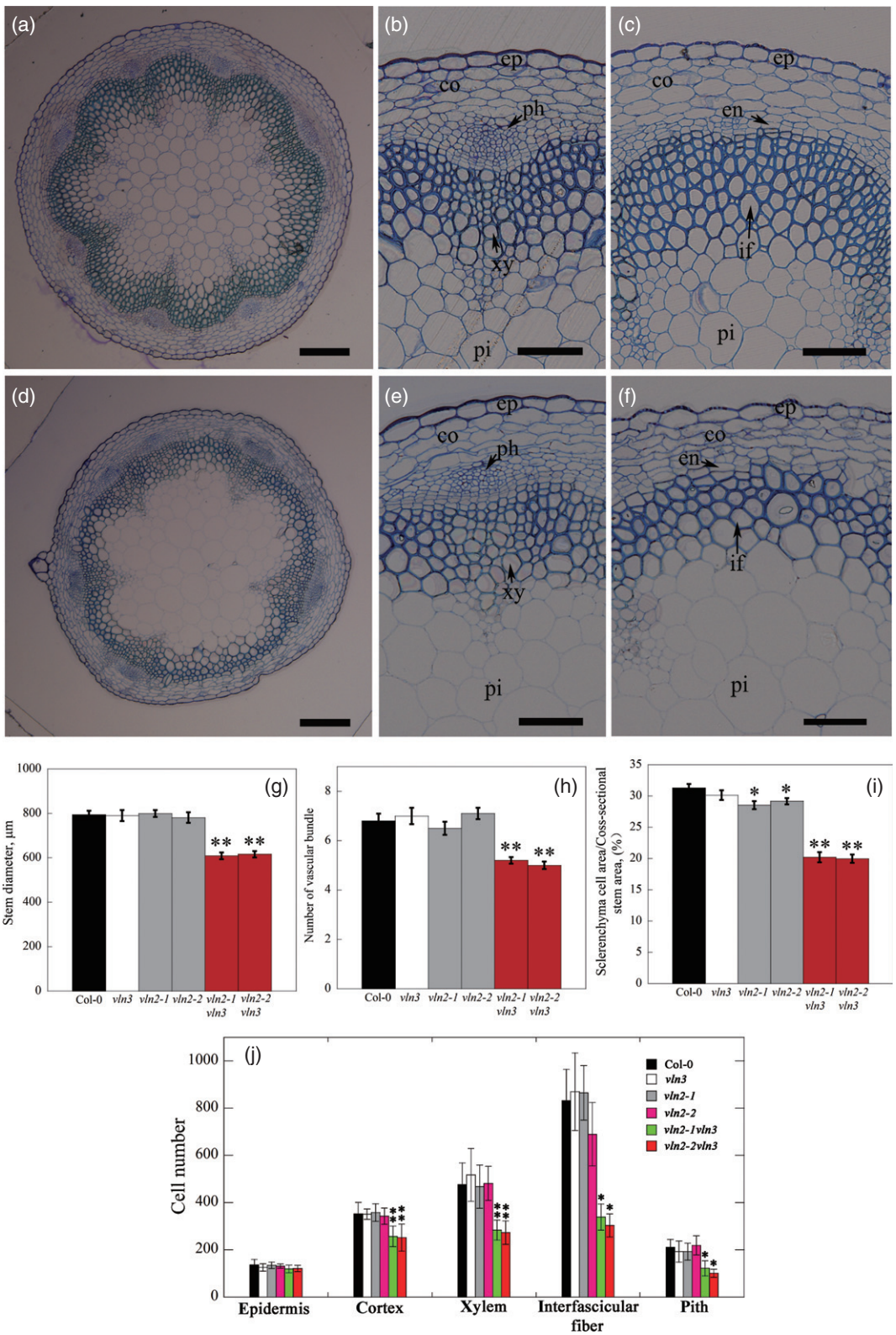

We initially examined the expression of several genes related to synthesis of secondary cell walls. Quantitative PCR analysis showed that loss of function of both *VLN2* and *VLN3* did not affect expression of the cellulose synthase genes *CesA7* and *CesA8* (Taylor *et al.*, 2003), the lignin biosynthetic genes *4CL1* (for hydroxycinnamate CoA ligase) and *CCoAOMT* (for caffeoyl CoA *O*-methyltransferase) (Boerjan *et al.*, 2003) (Figure S7A), implying that the secondary cell-wall synthesis machinery was not affected in *vln2 vln3* plants. Further, no obvious differences were detected between Col-0 (Figure S7B) and *vln2 vln3* plants (Figure S7C,D) when the secondary cell wall was visualized directly. To compare the difference in the secondary cell wall quantitatively, we measured the cell-wall thickness of inter-fascicular fiber cells. No significant difference in the thickness of secondary cell walls of inter-fascicular fibers cells was detected between Col-0 (1.64 $\pm$ 0.06 μm) and *vln2 vln3* double mutants (1.53 $\pm$ 0.09 μm for *vln2-1 vln3*; 1.8 $\pm$ 0.2 μm for *vln2-2 vln3*) (Figure S7E; $P = 0.578$ by one-way ANOVA analysis).

Loss of function of both *VLN2* and *VLN3* decreases the extent of actin filament bundling

We next examined whether the actin cytoskeleton was altered in the inflorescence stems of *vln2 vln3* plants. The cytoskeleton comprises mainly actin bundles in Col-0 xylem (Figure 4a), consistent with previous reports (Chaffey *et al.*, 2000; Gardiner *et al.*, 2003; Hu *et al.*, 2003; Zhong *et al.*, 2004, 2005a). However, the amount of thick actin bundles decreased substantially in *vln2 vln3* mutants (Figure 4a). More brighter and higher fluorescence peaks were detected in Col-0 (Figure 4b, upper panel) compared to the *vln2 vln3* double mutants (Figure 4b, lower panel), suggesting that VLN2 and VLN3 play an important role in bundling actin filaments *in vivo*. To assess quantitatively the effect of loss of function of *VLN2* and *VLN3* on bundling of actin filaments, we measured the skewness using the method developed by Higaki *et al.* (2010). Our measurement showed that the skewness of actin filaments decreased significantly from 4.92 $\pm$ 1.55 for Col-0 to 3.36 $\pm$ 0.71 and 3.43 $\pm$ 0.73 for *vln2-1 vln3* and *vln2-2 vln3*, respectively. Additionally, under identical image acquisition conditions, the overall fluorescence pixel intensities in the projected images were lower in *vln2-1 vln3* compared to Col-0 (Figure 4a), implying that VLN2 and VLN3 may be required for the stability of actin filaments. However, no obvious difference in actin organization was detected in either the *vln2* or *vln3* single mutants (Figure S8), suggesting that VLN2 and VLN3 act redundantly in actin organization. Collectively, these data suggest that VLN2 and VLN3 play important roles in bundling actin filaments in inflorescence stems, consistent with recently published results (Van der Honing *et al.*, 2012).

VLN2 binds to and bundles actin filaments and caps the barbed end of actin filaments

To determine the biochemical basis for the function(s) of VLN2 and VLN3, we studied their properties *in vitro*. Because VLN3 is well-documented biochemically (Khurana *et al.*,

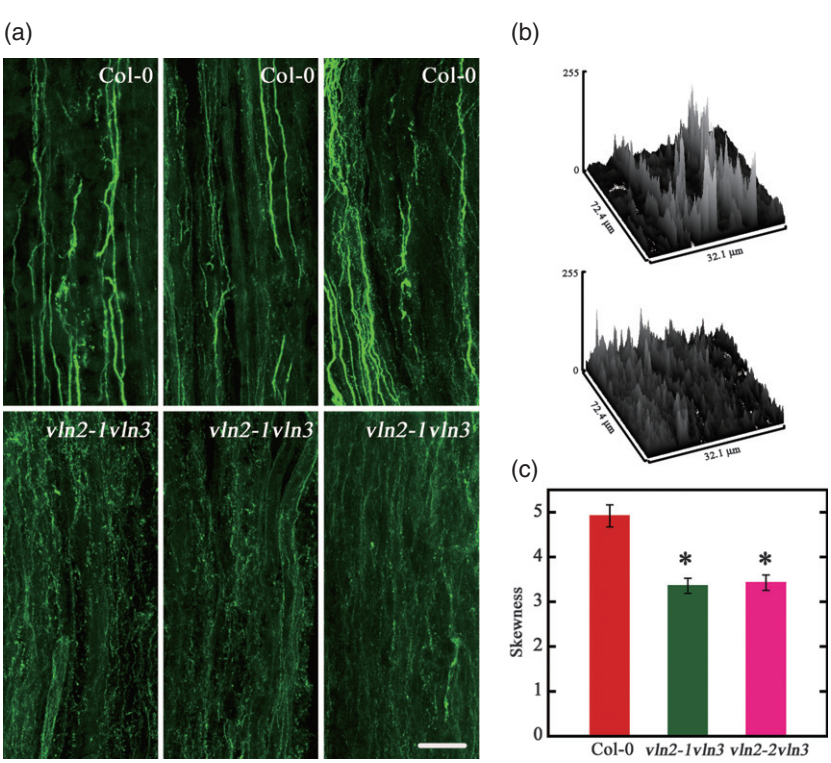

Figure 4. Thick longitudinal actin bundles are decreased markedly in the xylem fiber cells of *vln2 vln3* double mutant inflorescence stems.
(a) The main actin structures arranged longitudinally in both Col-0 and mutant xylem fiber cells. Compared with the Col-0 cells, actin bundles were thinner in *vln2-1 vln3* mutants. Scale bar = 10 μm.
(b) Three-dimensional graphs of the fluorescence pixel intensities of the entire image in the first column for Col-0 (top) and *vln2-1 vln3* (bottom) were generated using the 'Surface Plot' analysis tool in ImageJ software (http://rsbweb.nih.gov/ij/). Higher and brighter peaks correspond to thick bundles, and lower and darker peaks correspond to thin actin bundles.
(c) Skewness was measured to determine the degree of bundling in Col-0 and mutant xylem fiber cells. Values are means $\pm$ SD ($n \geq 14$). *$P < 0.05$ compared to Col-0 by Student's *t*-test.

2010), we put our efforts toward characterizing the biochemical activities of VLN2 *in vitro*. We generated recombinant protein in *Escherichia coli* and purified it to near homogeneity (Figure 5a). More VLN2 sedimented in the presence of actin filaments (Figure 5b, lane 4) compared to VLN2 alone (Figure 5b, lane 6) under high-speed centri-

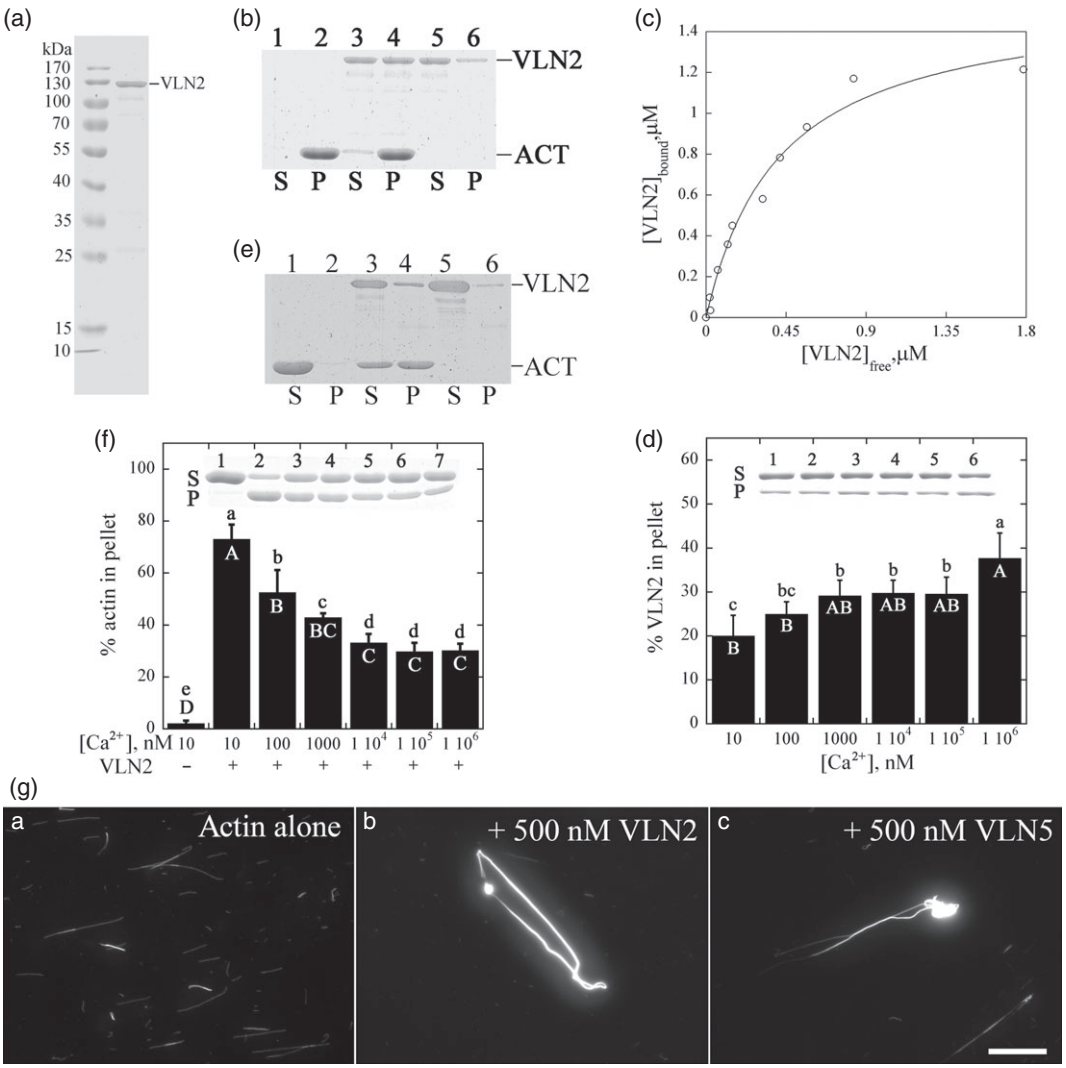

Figure 5. VLN2 binds to and bundles actin filaments.

(a) Coomassie blue-stained protein gel of recombinant VLN2 purified by affinity chromatography. Right lane, recombinant VLN2.

(b) A high-speed co-sedimentation assay was performed to examine binding of VLN2 to actin filaments. Lanes 1, 3 and 5, supernatants for actin alone, 3 μM actin + 0.5 μM VLN2, and 0.5 μM VLN2 alone, respectively. Lanes 2, 4 and 6, pellets for actin alone, 3 μM actin + 0.5 μM VLN2, and 0.5 μM VLN2 alone, respectively. S, supernatant; P, pellet.

(c) The amount of VLN2 in the pellet (bound) was plotted against the amount of VLN2 in the supernatant (free), and fitted with a hyperbolic function as described previously (Kovar *et al.*, 2000). A representative K_d value of 0.75 μM was obtained.

(d) Determination of VLN2 affinity for actin filaments in the presence of various concentrations of free calcium: 1 μM VLN2 was incubated with 3 μM F-actin in the presence of various concentrations of free calcium for 30 min at room temperature, the mixtures were then centrifuged at 100 000 ***g*** for 45 min, and the amount of VLN2 in the supernatant (S) and pellet (P) (inset) was quantified by densitometry. Error bars represent SD (n = 3). The statistical analysis was performed by one-way ANOVA followed by an Least Significant Difference post hoc multiple comparison; lower-case letters and capital letters indicate differences at $P < 0.05$ and $P < 0.01$, respectively.

(e) A low-speed co-sedimentation assay was performed to examine the bundling activity of VLN2. Lanes 1, 3 and 5, supernatants for actin alone, 3 μM actin + 1 μM VLN2, and 1 μM VLN2 alone, respectively. Lanes 2, 4 and 6, pellets for actin alone, 3 μM actin + 1 μM VLN2, and 1 μM VLN2 alone, respectively. S, supernatant; P, pellet.

(f) Determination of the bundling activity of VLN2 in the presence of various concentrations of free calcium: 1 μM VLN2 was incubated with 3 μM F-actin in the presence of various concentrations of free calcium for 30 min at room temperature, the mixtures were then centrifuged at 13 600 ***g*** for 45 min, and the amount of actin in the supernatant (S) and pellet (P) (inset) was quantified by densitometry. Error bars represent SD (n = 3). The statistical analysis was performed by one-way ANOVA followed by an Least Significant Difference post hoc multiple comparison; lower case letters and capital letters indicate differences at $P < 0.05$ and $P < 0.01$, respectively.

(g) Micrograph of actin filaments. Left, actin alone; middle, actin + 500 nM VLN2; right, actin + 500 nM VLN5. Scale bar = 10 μm.

fugation, suggesting that VLN2 binds to actin filaments. A dissociation constant value for the binding of VLN2 to actin filaments of 0.75 μM was calculated for the representative experiment in Figure 5(c), and a mean K_d of 1.3 ± 0.5 μM was determined from three independent experiments. Thus the VLN2 affinity for actin filaments is quite similar to that of VLN3 and VLN5 (Khurana *et al.*, 2010; Zhang *et al.*, 2010). We also determined VLN2 affinity for actin filaments in the presence of various concentrations of free calcium, and found that VLN2 binds to actin filaments with similar affinity across the physiological range of free calcium (Figure 5d).

We next decided to determine whether VLN2 can bundle actin filaments. The results showed that the amount of sedimented actin increased substantially in the presence of 500 nM VLN2 (Figure 5e, lane 4) compared to actin alone (Figure 5e, lane 2) under low-speed centrifugation, suggesting that VLN2 is able to form actin filament higher-order structures. Moreover, we found that the amount of sedimented actin decreased when the free calcium concentration was increased (Figure 5f). As the increase in calcium concentration did not decrease the affinity of VLN2 binding to actin filaments (Figure 5d), it may be that the elevation in the concentration of free calcium increased VLN2-mediated actin depolymerization, which probably resulted from both VLN2-mediated filament severing and barbed end capping (see below). The bundling activity of VLN2 was further examined by visualizing actin filaments directly with a fluorescence microscope. Most actin filaments behave as single filaments in the absence of villins (Figure 5g, left). However, in the presence of VLN2, actin filaments were organized into large bundles (Figure 5g, middle). VLN5 (Zhang *et al.*, 2010) was used as a positive control (Figure 5g, right). Taken together, these results suggest that VLN2, like VLN3 and VLN5 (Khurana *et al.*, 2010; Zhang *et al.*, 2010), binds to and bundles actin filaments.

A seeded actin elongation assay was then performed to test whether VLN2 caps the barbed end of actin filaments. VLN2 inhibited actin elongation in a dose-dependent manner (Figure S9A). A representative K_d value of 9.4 nM was calculated by fitting the data in Figure S7A to equation 1 (Figure S9B). A mean K_d value of 9.4 ± 1.4 nM was calculated from three independent experiments. We also determined whether the variation in calcium concentration affected the affinity of VLN2 for the barbed end of actin filaments, and found that the inhibitory effect of VLN2 on actin elongation increased while the free calcium concentration was elevated (Figure S9C), implying that the capping activity may be regulated by calcium. Again, given that the filament-severing activity of VLN2 increased with the elevation of free calcium (see below), the contribution of VLN2-mediated filament severing activity cannot be ruled out. A dilution-mediated actin depolymerization assay was then performed to test whether VLN2 stabilized actin filaments. VLN2 prevented actin depolymerization in a dose-dependent manner (Figure S9D), confirming its effect in stabilizing actin filaments.

VLN2 severs actin filaments

With Arabidopsis VLN1 as a notable exception (Huang *et al.*, 2005), three other Arabidopsis VLNs have been reported to have calcium-dependent actin filament-severing activity (Khurana *et al.*, 2010; Zhang *et al.*, 2010, 2011). As shown in Figure 6(a), no obvious breaks along actin filaments were detected after introduction of buffer only (see also Video Clip S1). However, after perfusion of 1 nM VLN2 in the presence of 1 μM Ca^{2+}, numerous breaks along actin filaments were detected (Figure 6b and Video Clip S2), and an increasing number of breaks were detected after the concentration of VLN2 was increased (Figure 6d, Table S1 and Video Clips S2 and S3), suggesting that VLN2 severs actin filaments in a dose-dependent manner. To determine the threshold of calcium concentration required for severing activity, 1 nM VLN2 and various concentrations of free Ca^{2+} were introduced into the perfusion chamber. After free [Ca^{2+}] was elevated to 1 μM, the actin filament-severing activity of VLN2 was very prominent (Figure 6c, Table S1, and Video Clips S2, S4 and S5), implying that the actin filament-severing activity of VLN2 is biologically relevant. The severing frequency is much greater than that of VLN3 and VLN5 (Khurana *et al.*, 2010; Zhang *et al.*, 2010). Taken together, these results suggest that VLN2 severs actin filaments in a dose-dependent manner, and that physiological Ca^{2+} levels are sufficient to trigger severing activity.

DISCUSSION

In contrast to the restricted expression of mammalian villins in absorptive tissues, Arabidopsis *VLN* genes are expressed in most tissues (Klahre *et al.*, 2000; Khurana *et al.*, 2010; Zhang *et al.*, 2010; this study). This indicates that villin-like proteins may serve a more general function in actin dynamics in Arabidopsis than in mammalian systems (Klahre *et al.*, 2000). Moreover, villin-like genes have been found only in multicellular organisms, and no homolog has been identified from the single-celled budding yeast *Saccharomyces cerevisiae*, which indicates that villin-like genes may only have emerged with the emergence of multicellular organisms during evolution.Using Arabidopsis as an experimental system may allow us to dissect the function of villins during complex developmental processes. Additionally, the presence of a multi-gene family with overlapping expression patterns allows us to test whether the villin isovariants function redundantly or whether they have distinct functions, or both.

Here we have shown that two widely expressed and closely related villin isovariants from Arabidopsis, VLN2 and VLN3, act redundantly during sclerenchyma development in inflorescence stems. To our knowledge, there have been no studies showing that direct genetic manipulation of the actin

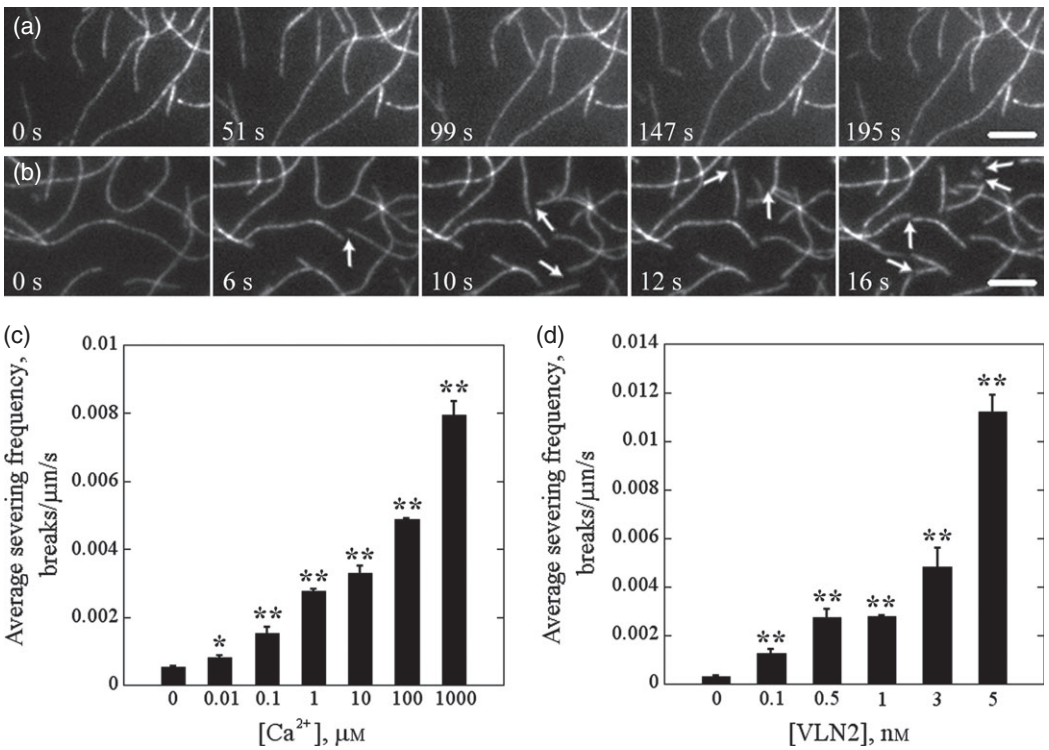

Figure 6. Direct visualization of the actin filament-severing activity of VLN2 by time-lapse TIRFM.
(a, b) Rhodamine-actin filaments at 50 nM were introduced into a perfusion chamber pre-coated with *N*-ethylmaleimide-myosin. It was subsequently perfused with control TIRF buffer (10 mM imidazole, pH 7.0, 50 mM KCl, 1 mM EGTA, 1 mM MgCl2, 100 mM DTT, 0.2 mM ATP, 15 mM glucose, 0.4 mg/mL glucose oxidase, 0.08 mg/mL catalase, 0.2% BSA, and 0.5% methylcellulose) (a) or 1 nM VLN2 (b) in the presence of 1 μM free Ca^{2+}. Time-lapse images were collected at 1 or 3 s intervals. Individual actin filaments showed an increasing number of breaks (indicated by arrows). Scale bar = 5 μm. See also Video Clips S1 and S2.
(c) The severing activity of VLN2 is Ca^{2+}-dependent: 1 nM VLN2 in the presence of various concentrations of Ca^{2+} was introduced into a perfusion chamber containing 50 nM rhodamine-actin filaments, and time-lapse images were collected. Ten filaments for each experimental treatment were counted, and the mean severing frequency (number of breaks μm^{-1} s^{-1}) was plotted against the concentration of Ca^{2+}. The experiment was repeated three times. Values are means ± SE; $*P < 0.05$ and $**P < 0.01$ compared to 0 μM Ca^{2+} by Student's *t* test.
(d) VLN2 severs actin filaments in a dose-dependent manner. Various concentrations of VLN2 in the presence of 1 μM Ca^{2+} were perfused into chambers containing 50 nM rhodamine-actin filaments, and time-lapse images were collected. Ten filaments for each experimental treatment were counted, and the mean severing frequencies were plotted against the concentration of VLN2. The experiment was repeated three times. Values are means ± SE; $**P < 0.01$ compared to 0 nM VLN2 by Student's *t*-test.

cytoskeleton impairs vascular development. Therefore, our study opens an avenue for future work on this important topic.

VLN2 is a versatile actin-modifying protein and is important for actin filament bundling *in vivo*

Five villin-like genes are encoded in the Arabidopsis genome (Klahre *et al.*, 2000; Huang *et al.*, 2005), and their encoded proteins have been characterized biochemically *in vitro*. With the exception of VLN1, which is a simple actin bundler (Huang *et al.*, 2005; Khurana *et al.*, 2010), the other four villin isovariants have now been demonstrated to cap, sever and bundle actin filaments (this study; Khurana *et al.*, 2010; Zhang *et al.*, 2010, 2011). The fact that VLN2 retains the full suite of actin-modifying activities may be due to a general conservation of actin-binding residues (Huang *et al.*, 2005). Consistent with the biochemical properties of VLN2 and VLN3, loss of function of *VLN2* and *VLN3 in planta* led to a decrease in the amount of F-actin bundling in inflorescence stems (Figure 4) (Van der Honing *et al.*, 2012). These results are similar to the previous demonstration that injection of 135-ABP antibody induces the breakdown of transvacuolar strands and thinning of actin filament bundles in transvacuolar strands of root hairs (Tominaga *et al.*, 2000). Our data, together with recently published data (Van der Honing *et al.*, 2012), provide further direct genetic evidence showing that the villin family is indeed a major player in bundling actin filaments throughout the plant and during development.

In addition to organization of actin filaments into bundles and networks, the dynamic reorganization of individual actin filaments is also important for cytoskeletal function. Rapid actin turnover and actin filament severing are key dynamic features in the cortical array of epidermal cells (Staiger *et al.*, 2009; Smertenko *et al.*, 2010; Henty *et al.*, 2011). Direct visualization of actin filaments by TIRFM *in vitro* demonstrated unambiguously that VLN2 (this study) and VLN3

(Khurana *et al.*, 2010) sever actin filaments in the presence of micromolar free calcium (Figure 6; see also Video Clips S2, S3 and S5). This suggests that the severing activity of VLN2 may be biologically relevant, especially in situations where cytosolic calcium is elevated. It is fair to postulate that, as for the recent demonstration of severing by an ADF (actin-depolymerizing factor) family member *in vivo* (Henty *et al.*, 2011), VLN2 and VLN3 may make an important contribution to single actin filament dynamics.

VLN2 and VLN3 are involved in the development of sclerenchyma

How the development of sclerenchyma is regulated remains largely unknown. Previous studies showed that various factors are involved in regulating the differentiation and proliferation of vascular cells, including hormones, transcription factors and the cytoskeleton (Ye *et al.*, 2002; Turner *et al.*, 2007; Demura and Ye, 2010; Ohashi-Ito and Fukuda, 2010). The role of microtubules during vascular development has been studied quite intensively. Our current view is that cortical microtubules guide the movement of cellulose synthase (CesA) complexes during deposition of microfibrils (Emons *et al.*, 2007; Lloyd and Chan, 2008), consequently controlling the synthesis of secondary cell walls and cell expansion. Microtubules may also coordinate and regulate the delivery of CesA-containing vesicles to the plasma membrane (Crowell *et al.*, 2009; Gutierrez *et al.*, 2009). However, by comparison, the role of the actin cytoskeleton during vascular development is rather poorly understood.

Previous visualization of the actin cytoskeleton showed that actin cables are arranged longitudinally during tracheary element differentiation (Chaffey *et al.*, 2000; Gardiner *et al.*, 2003), suggesting that bundled actin may play an important role in this process by serving as tracks for the vesicular trafficking of cell-wall components. Indeed, live cell imaging of actin filaments and cellulose synthase complexes (CSCs) demonstrated that actin cables are essential for the rapid trafficking of CSCs around cells (Wightman and Turner, 2008). Additionally, previous studies showed that actin cables regulated the positioning of Golgi apparatus containing CesA (Crowell *et al.*, 2009; Gutierrez *et al.*, 2009), which may indirectly control where CesA is inserted in the plasma membrane. Several studies provide circumstantial evidence for this. Analysis of several Arabidopsis mutants with thin secondary cell walls, including *fra3* (with a mutation in an inositol polyphosphate 5-phosphatase), *fra4* (with a mutation in a protein containing a GTP-binding motif) and *fra7* (with a mutation in a phosphoinositide phosphastase), showed that actin cables become disorganized (Hu *et al.*, 2003; Zhong *et al.*, 2004, 2005a). These studies provide indirect evidence that actin filaments play an important role in regulating the synthesis of secondary cell walls, but do not establish cause and effect. Although the relationship between actin disorganization and reduced secondary cell-wall synthesis is unclear, the authors reasoned that the alteration of actin dynamics may reduce the trafficking of cell-wall components in these mutants (Hu *et al.*, 2003; Zhong *et al.*, 2004, 2005a). However, to date, there have been no studies that demonstrate that direct genetic manipulation of the actin cytoskeleton alters the development of sclerenchyma.

Several lines of evidence showed that development of sclerenchyma was affected in *vln2 vln3* double mutants. Close examination of the anatomy of inflorescence stems revealed that the width of the stems and the number of vascular bundles was significantly reduced in *vln2 vln3* mutants (Figure 3i). Further examination showed that the percentage of sclerenchyma cells was decreased in *vln2 vln3* double mutants (Figure 3j). Consistent with their roles in maintaining plant mechanical strength, the force needed to pull the inflorescence stems apart decreased significantly in *vln2 vln3* plants (Figure 2), which explains well the appearance of a pendent phenotype in these plants. Previous analyses of several vascular development mutants revealed a correlation with defects in secondary cell-wall synthesis (Hu *et al.*, 2003; Zhong *et al.*, 2005a, 2006; Ohashi-Ito *et al.*, 2010), which inspired us to examine whether secondary cell-wall properties were altered in *vln2 vln3* plants. Our initial observations showed that the secondary cell-wall synthesis machinery may not be altered in *vln2 vln3* plants (Figure S7). Further evidence showed that there is no significant difference in the thickness of secondary cell walls from inter-fascicular fibers between Col-0 and *vln2 vln3* plants (Figure S7). This implies that delivery of non-cellulosic cell-wall polysaccharides by secretion may not be altered in *vln2 vln3* double mutants.

How exactly the loss of function of *VLN2* and *VLN3* induced defects in the development of sclerenchyma deserves further study. Loss of function of *VLN2* and *VLN3* did not affect the deposition of secondary cell walls, distinguishing *vln2 vln3* double mutants from previously identified vascular development mutants (Zhong *et al.*, 1997, 2004, 2005b, 2006; Hu *et al.*, 2003; Ohashi-Ito *et al.*, 2010). Therefore, these double mutant lines may provide good experimental material to explore further the relationship between the actin cytoskeleton and vascular tissue development. In addition, loss of function of *VLN2* and *VLN3* did not induce isotropic cell expansion, further distinguishing *vln2 vln3* double mutants from previously identified vascular development mutants resulting from mutations that affect the microtubule system (Burk *et al.*, 2001; Zhong *et al.*, 2002; Pesquet *et al.*, 2010). Collectively, our study provides key direct genetic evidence that the actin cytoskeleton is involved in the development of sclerenchyma, including inter-fascicular fibers and vascular bundles.

Although we found that the extent of actin filament bundling decreased (Figure 4), the cell length of inter-fascicular fiber cells was not affected in *vln2 vln3* double

mutants (Figure S6), suggesting that organization of the actin cytoskeleton or the extent of filament bundling may not be a direct regulator of cell elongation. Consistent with this, previous measurements of single actin filament dynamics in etiolated hypocotyls showed that actin filament elongation rates and severing frequencies were not quantitatively different when axially expanding and non-growing epidermal cells were compared (Staiger *et al.*, 2009). However, in contrast to this finding, a similar study showed that loss of function of *VLN2* and *VLN3* affected cell elongation of root epidermal cells (Van der Honing *et al.*, 2012), implying that VLN2- and VLN3- mediated actin dynamics and/or organization have different effects on cell elongation depending on cell type, consistent with recent findings showing that loss of function of *ADF4* increases actin filament bundling in hypocotyl and petiolar epidermal cells, but has an opposite effect on the growth of those two types of epidermal cells. (Henty *et al.*, 2011).

Our results showed that the number of sclerenchyma cells, cortex cells and pith cells decreased significantly in *vln2 vln3* inflorescence stems (Figure 3j), implying that cell division may be altered in *vln2 vln3* mutants. Therefore, VLN2- and VLN3-mediated actin dynamics and organization may be important in regulating the progression of cell division. This supports previous findings that the actin cytoskeleton plays a role in cell division. For instance, pharmacological disruption of the actin cytoskeleton affects cell division (Hoshino *et al.*, 2003; Sano *et al.*, 2005). However, the role of actin filaments during cell division is relatively less well explored than that of microtubules. In particular, the effect of actin drugs on cell division is less potent compared to that of microtubule drugs (Hoshino *et al.*, 2003; Sano *et al.*, 2005; Vanstraelen *et al.*, 2006), suggesting that the function of the actin cytoskeleton during cell division may be auxiliary to that of microtubules. How the dysfunction of the actin cytoskeleton in *vln2 vln3* double mutants affects cell division in inflorescence stems requires further research.

In summary, this work shows that two widely expressed and closely related Arabidopsis *VILLIN* genes, *VLN2* and *VLN3*, are redundantly required for proper sclerenchyma development and the upright growth habit of inflorescence stems. *In vitro* biochemical analyses indicate that VLN2 and VLN3 may directly participate in these physiological processes via stabilization and bundling of actin filaments.

EXPERIMENTAL PROCEDURES

Plant materials and growth conditions

Three T-DNA insertion mutants [SAIL_613_C03 (*vln2-1*), SAIL_813_H02 (*vln2-2*) and SALK_078340 (*vln3*)] were obtained from the Arabidopsis Biological Resource Center. To genotype the T-DNA insertion lines, PCR was performed using the isolated genomic DNA as the template with gene-specific primers (see Table S2). The *vln2 vln3* double mutant lines were generated by crossing either *vln2-1* or *vln2-2* with *vln3*. The generation of *VLN2* and *VLN3* complementary lines, and the detection of transcription levels of relative genes are described in Data S1. Arabidopsis seeds were sown on solid medium containing half-strength Murashige and Skoog salts with 5 mM MES (pH 5.5), 10 g L^{-1} sucrose and 15 g L^{-1} agar, and cultured vertically for seedling phenotypic analysis or grown in soil in the growth chamber under a light/dark cycle of 16/8 h at 20–22°C. *Arabidopsis thaliana* ecotype Columbia was used as the wild-type control (Col-0).

Tissue sections and microscopy analysis

For transmission electron microscopy (TEM) analysis, basal segments of the primary inflorescence stems of 7-week-old plants were pre-fixed in 2.5% glutaraldehyde in 0.1 M phosphate buffer (pH 7.2) and post-fixed in 1% osmium tetraoxide. Specimens were embedded in Spurr's resin and cut with a microtome (Leica Ultracut R; http://www.leica-microsystems.com) into 50 nm thick cross-sections. Samples were stained with uranyl acetate and lead citrate, and observed under a transmission electron microscope (Hitachi 7500; http://www.hitachi.com). For transverse and longitudinal semi-thin section preparations, samples were fixed in FAA buffer (formaldehyde:glacial acetic acid:50% ethanol, 1:1:18). Embedded specimens were cut into 1 μm thick sections, stained with 0.05% toluidine blue and observed under an optical microscope (Olympus BX51; http://www.olympusamerica.com). Hand-cut stem sections (50–100 μm thick) were stained with phloroglucinol HCl for lignin. The lignified cells appear as red areas in Figure S5.

Measurement of the breaking force

The basal part of inflorescence stems of 7-week-old plants of Col-0 and *VLN2* and/or *VLN3* T-DNA insertion mutants were used for the measurements. The ends of each stem segment were clamped at the same distance between two clamps and torn apart at the same speed. The force required to break the samples was recorded by a microtester (55R1122; INSTRON, http://www.instron.us/wa/home/default_en.aspx). Twelve plants of each genotype were examined, and all samples were treated under identical conditions.

Actin staining and microscopy analysis

Immunostaining of actin structures in inflorescence stems was carried out as described by Zhong *et al.* (2004) with minor modifications. Briefly, segments of the upper region of 5-week-old main stems were fixed with 4% paraformaldehyde and 0.5% glutaraldehyde in PME buffer (50 mM PIPES, 5 mM $MgSO_4$, 5 mM EGTA, pH 7.0) containing 0.05% v/v Triton X-100. Fixed samples were cut longitudinally into thin sections and processed using the following procedures. Specimens were incubated with the primary antibody (anti-actin for plants; Abmart Inc., http://www.abmart.cn), and subsequently incubated with the secondary antibody (Alexa Fluor® 488 goat anti-mouse IgG; Invitrogen, http://www.invitrogen.com). Observation of actin structure was performed using a Leica TCS SP5 laser scanning confocal microscope equipped with a water immersion objective (HCX PL APO 63 × /1.2 W). The fluorescence was excited using the 488 nm line of an argon laser, optical Z-series sections were collected at 0.5 μm steps (three-line averaging and one-frame averaging), and the images are projections of the collected Z-series.

Skewness analysis of actin bundling

Skewness analysis of actin bundling was mainly performed as described by Higaki *et al.* (2010). Briefly, obvious noisy signals in the Z-series images were first eliminated manually plane by plane. Then the rolling ball radius when subtracting background was set to 15

pixels and Gaussian blurring was set to 1. Then the stack images were skeletonized and projected with maximum intensity. The projected images were used to measure the skewness value.

Protein production

The VLN2 coding sequence was amplified using primers *VLN2*-CDS-F and *VLN2*-CDS-R (see Table S2) using the full-length *VLN2* cDNA clone (pda07649) as the template. After verification by sequence analysis, the pET23a-VLN2 construct was created by inserting the VLN2 full-length cDNA into pET23a vector (http://www.emdmillipore.com/chemicals) digested with *Not*I/*Xho*I. The pET23a-VLN2 vector was introduced into the BL21 (DE3) strain of *E. coli*. After induction by addition of 0.4 mM isopropyl β-D-thiogalactopyranoside overnight at 16°C, cells were collected and resuspended in binding buffer (25 mM Tris/HCl, pH 8.0, 5 mM imidazole, 250 mM KCl, 0.01% NaN_3, 1 mM DTT) supplemented with protease inhibitor cocktail (Roche, http://www.roche.com) and sonicated. VLN2 was subsequently purified using Ni-NTA resin (Qiagen, http://www.qiagen.com) according to the manufacturer's instructions. The eluted protein was dialyzed against 10 mM Tris/HCl pH 8.0, 0.01% NaN_3, 1 mM DTT. The protein was aliquoted and flash-frozen in liquid nitrogen and stored at −80°C. The protein was clarified at 200 000 ***g*** for 30 min before use, and the concentration was determined with the Bradford assay with bovine serum albumin as a standard. Human profilin, VLN5 and muscle actin were purified as described by Spudich and Watt (1971), Pollard (1984) and Fedorov *et al.* (1994). Actin was further labeled with either pyrene iodoacetamide or 5-(and 6)-carboxytetramethylrhodamine, succinimidyl ester as described by Pollard (1984) and Amann and Pollard (2001).

Biochemical characterization of VLN2 *in vitro*

Low-speed and high-speed F-actin co-sedimentation assays were performed as described by Kovar *et al.* (2000). Pyrene actin-based kinetic assays to determine the barbed end capping and stabilizing activity of VLN2 were performed as described by Zhang *et al.* (2010). Direct visualization of actin bundle formation by fluorescence light microscopy was performed as described by Huang *et al.* (2005). Direct visualization of actin filament-severing by TIRFM was performed exactly as described by Zhang *et al.* (2010).

ACKNOWLEDGEMENTS

We thank the Arabidopsis Biological Resource Center and the Nottingham Arabidopsis Stock Centre for providing T-DNA insertion lines, and RIKEN for the full-length cDNA. We especially thank Christopher J. Staiger, Department of Biological Sciences, Purdue University, West Lafayette, IN, USA) for his constructive comments and help with the manuscript writing. This work was supported by grants from the National Natural Science Foundation of China (31121065 and 31071179). S.H. was supported by the Chinese Academy of Sciences through its One Hundred Talents Program and China National Funds for Distinguished Young Scholars (31125004).

SUPPORTING INFORMATION

Additional Supporting Information may be found in the online version of this article:

Figure S1. *VLN2* and *VLN3* are expressed widely in Arabidopsis tissues.

Figure S2. The phenotypes of *vln2 vln3* mutants are complemented by expression of either *VLN2* or *VLN3.*

Figure S3. Sclerenchyma development is not affected in *vln2* or *vln3* single mutants.

Figure S4. Schematic representation of the method used to determine the proportion of sclerenchyma cells in the inflorescence stem.

Figure S5. The development of sclerenchyma is affected in *vln2 vln3* mutant inflorescence stems.

Figure S6. Loss of function of *VLN2* and *VLN3* does not affect the length of inter-fascicular fiber cells.

Figure S7. Loss of function of *VLN2* and *VLN3* does not affect the thickness of the secondary cell wall.

Figure S8. Loss of function of either *VLN2* or *VLN3* does not obviously alter the main actin structure in the xylem fiber cells.

Figure S9. VLN2 caps the barbed end of actin filaments.

Table S1. Quantification of VLN2-mediated actin filament-severing frequency.

Table S2. Primer pairs used in this study.

Video Clip S1. Time-lapse TIRFM series of actin filaments treated with 1 × TIRF buffer containing 1 μM free Ca^{2+}.

Video Clip S2. Time-lapse TIRFM series of actin filaments exposed to 1 nM VLN2 in the presence of 1 μM Ca^{2+}.

Video Clip S3. Time-lapse TIRFM series of actin filaments exposed to 5 nM VLN2 in the presence of 1 μM Ca^{2+}.

Video Clip S4. Time-lapse TIRFM series of actin filaments exposed to 1 nM VLN2 without Ca^{2+}.

Video Clip S5. Time-lapse TIRFM series of actin filaments exposed to 1 nM VLN2 in the presence of 100 μM Ca^{2+}.

Data S1. Complementation, RT-PCR and real-time PCR analysis.

Please note: As a service to our authors and readers, this journal provides supporting information supplied by the authors. Such materials are peer-reviewed and may be re-organized for online delivery, but are not copy-edited or typeset. Technical support issues arising from supporting information (other than missing files) should be addressed to the authors.

REFERENCES

Amann, K.J. and Pollard, T.D. (2001) The Arp2/3 complex nucleates actin filament branches from the sides of pre-existing filaments. *Nat. Cell Biol.* **3**, 306–310.

Boerjan, W., Ralph, J. and Baucher, M. (2003) Lignin biosynthesis. *Annu. Rev. Plant Biol.* **54**, 519–546.

Bretscher, A. and Weber, K. (1979) Villin: The major microfilament-associated protein of the intestinal microvillus. *Proc. Natl Acad. Sci. USA*, **76**, 2321–2325.

Burk, D.H., Liu, B., Zhong, R., Morrison, W.H. and Ye, Z.H. (2001) A katanin-like protein regulates normal cell wall biosynthesis and cell elongation. *Plant Cell*, **13**, 807–827.

Chaffey, N., Barlow, P. and Barnett, J. (2000) A cytoskeletal basis for wood formation in angiosperm trees: The involvement of microfilaments. *Planta*, **210**, 890–896.

Crowell, E.F., Bischoff, V., Desprez, T., Rolland, A., Stierhof, Y.D., Schumacher, K., Gonneau, M., Hofte, H. and Vernhettes, S. (2009) Pausing of Golgi bodies on microtubules regulates secretion of cellulose synthase complexes in *Arabidopsis*. *Plant Cell*, **21**, 1141–1154.

Demura, T. and Ye, Z.H. (2010) Regulation of plant biomass production. *Curr. Opin. Plant Biol.* **13**, 299–304.

Emons, A.M., Hofte, H. and Mulder, B.M. (2007) Microtubules and cellulose microfibrils: How intimate is their relationship? *Trends Plant Sci.* **12**, 279–281.

Fedorov, A.A., Pollard, T.D. and Almo, S.C. (1994) Purification, characterization and crystallization of human platelet profilin expressed in *Escherichia coli*. *J. Mol. Biol.* **241**, 480–482.

Ferrary, E., Cohen-Tannoudji, M., Pehau-Arnaudet, G. *et al.* (1999) *In vivo*, villin is required for Ca^{2+}-dependent F-actin disruption in intestinal brush borders. *J. Cell Biol.* **146**, 819–830.

Friederich, E., Huet, C., Arpin, M. and Louvard, D. (1989) Villin induces microvilli growth and actin redistribution in transfected fibroblasts. *Cell*, **59**, 461–475.

Friederich, E., Pringault, E., Arpin, M. and Louvard, D. (1990) From the structure to the function of villin, an actin-binding protein of the brush border. *BioEssays*, **12**, 403–408.

Gardiner, J.C., Taylor, N.G. and Turner, S.R. (2003) Control of cellulose synthase complex localization in developing xylem. *Plant Cell*, **15**, 1740–1748.
Gutierrez, R., Lindeboom, J.J., Paredez, A.R., Emons, A.M. and Ehrhardt, D.W. (2009) *Arabidopsis* cortical microtubules position cellulose synthase delivery to the plasma membrane and interact with cellulose synthase trafficking compartments. *Nat. Cell Biol.* **11**, 797–806.
Henty, J.L., Bledsoe, S.W., Khurana, P., Meagher, R.B., Day, B., Blanchoin, L. and Staiger, C.J. (2011) *Arabidopsis* actin depolymerizing factor4 modulates the stochastic dynamic behavior of actin filaments in the cortical array of epidermal cells. *Plant Cell*, **23**, 3711–3726.
Higaki, T., Kutsuna, N., Sano, T., Kondo, N. and Hasezawa, S. (2010) Quantification and cluster analysis of actin cytoskeletal structures in plant cells: Role of actin bundling in stomatal movement during diurnal cycles in *Arabidopsis* guard cells. *Plant J.* **61**, 156–165.
Hoshino, H., Yoneda, A., Kumagai, F. and Hasezawa, S. (2003) Roles of actin-depleted zone and preprophase band in determining the division site of higher-plant cells, a tobacco BY-2 cell line expressing GFP–tubulin. *Protoplasma*, **222**, 157–165.
Hruz, T., Laule, O., Szabo, G., Wessendorp, F., Bleuler, S., Oertle, L., Widmayer, P., Gruissem, W. and Zimmermann, P. (2008) Genevestigator v3: A reference expression database for the meta-analysis of transcriptomes. *Adv. Bioinformatics*, **2008**, 420747.
Hu, Y., Zhong, R., Morrison, W.H. III and Ye, Z.H. (2003) The *Arabidopsis RHD3* gene is required for cell wall biosynthesis and actin organization. *Planta*, **217**, 912–921.
Huang, S., Robinson, R.C., Gao, L.Y., Matsumoto, T., Brunet, A., Blanchoin, L. and Staiger, C.J. (2005) *Arabidopsis* VILLIN1 generates actin filament cables that are resistant to depolymerization. *Plant Cell*, **17**, 486–501.
Khurana, S. and George, S.P. (2008) Regulation of cell structure and function by actin-binding proteins: Villin's perspective. *FEBS Lett.* **582**, 2128–2139.
Khurana, P., Henty, J.L., Huang, S., Staiger, A.M., Blanchoin, L. and Staiger, C.J. (2010) *Arabidopsis* VILLIN1 and VILLIN3 have overlapping and distinct activities in actin bundle formation and turnover. *Plant Cell*, **22**, 2727–2748.
Klahre, U., Friederich, E., Kost, B., Louvard, D. and Chua, N.H. (2000) Villin-like actin-binding proteins are expressed ubiquitously in *Arabidopsis*. *Plant Physiol.* **122**, 35–48.
Kovar, D.R., Staiger, C.J., Weaver, E.A. and McCurdy, D.W. (2000) AtFim1 is an actin filament crosslinking protein from *Arabidopsis thaliana*. *Plant J.* **24**, 625–636.
Lloyd, C. and Chan, J. (2008) The parallel lives of microtubules and cellulose microfibrils. *Curr. Opin. Plant Biol.* **11**, 641–646.
Ma, L., Sun, N., Liu, X., Jiao, Y., Zhao, H. and Deng, X.W. (2005) Organ-specific expression of *Arabidopsis* genome during development. *Plant Physiol.* **138**, 80–91.
Mahajan-Miklos, S. and Cooley, L. (1994) The villin-like protein encoded by the Drosophila *quail* gene is required for actin bundle assembly during oogenesis. *Cell*, **78**, 291–301.
Matova, N., Mahajan-Miklos, S., Mooseker, M.S. and Cooley, L. (1999) *Drosophila* Quail, a villin-related protein, bundles actin filaments in apoptotic nurse cells. *Development*, **126**, 5645–5657.
Matsudaira, P.T. and Burgess, D.R. (1979) Identification and organization of the components in the isolated microvillus cytoskeleton. *J. Cell Biol.* **83**, 667–673.
McGough, A.M., Staiger, C.J., Min, J.K. and Simonetti, K.D. (2003) The gelsolin family of actin regulatory proteins: Modular structures, versatile functions. *FEBS Lett.* **552**, 75–81.
Nakayasu, T., Yokota, E. and Shimmen, T. (1998) Purification of an actin-binding protein composed of 115-kDa polypeptide from pollen tubes of lily. *Biochem. Biophys. Res. Commun.* **249**, 61–65.
Ohashi-Ito, K. and Fukuda, H. (2010) Transcriptional regulation of vascular cell fates. *Curr. Opin. Plant Biol.* **13**, 670–676.
Ohashi-Ito, K., Oda, Y. and Fukuda, H. (2010) *Arabidopsis* VASCULAR-RELATED NAC-DOMAIN6 directly regulates the genes that govern programmed cell death and secondary wall formation during xylem differentiation. *Plant Cell*, **22**, 3461–3473.
Pesquet, E., Korolev, A.V., Calder, G. and Lloyd, C.W. (2010) The microtubule-associated protein AtMAP70-5 regulates secondary wall patterning in *Arabidopsis* wood cells. *Curr. Biol.* **20**, 744–749.
Pollard, T.D. (1984) Polymerization of ADP-actin. *J. Cell Biol.* **99**, 769–777.
Pollard, T.D. and Cooper, J.A. (2009) Actin, a central player in cell shape and movement. *Science*, **326**, 1208–1212.
Sano, T., Higaki, T., Oda, Y., Hayashi, T. and Hasezawa, S. (2005) Appearance of actin microfilament 'twin peaks' in mitosis and their function in cell plate formation, as visualized in tobacco BY-2 cells expressing GFP–fimbrin. *Plant J.* **44**, 595–605.
Silacci, P., Mazzolai, L., Gauci, C., Stergiopulos, N., Yin, H.L. and Hayoz, D. (2004) Gelsolin superfamily proteins: Key regulators of cellular functions. *Cell. Mol. Life Sci.* **61**, 2614–2623.
Smertenko, A.P., Deeks, M.J. and Hussey, P.J. (2010) Strategies of actin reorganisation in plant cells. *J. Cell Sci.* **123**, 3019–3028.
Spudich, J.A. and Watt, S. (1971) The regulation of rabbit skeletal muscle contraction. I. Biochemical studies of the interaction of the tropomyosin–troponin complex with actin and the proteolytic fragments of myosin. *J. Biol. Chem.* **246**, 4866–4871.
Staiger, C.J. and Blanchoin, L. (2006) Actin dynamics: old friends with new stories. *Curr. Opin. Plant Biol.* **9**, 554–562.
Staiger, C.J., Sheahan, M.B., Khurana, P., Wang, X., McCurdy, D.W. and Blanchoin, L. (2009) Actin filament dynamics are dominated by rapid growth and severing activity in the *Arabidopsis* cortical array. *J. Cell Biol.* **184**, 269–280.
Staiger, C.J., Poulter, N.S., Henty, J.L., Franklin-Tong, V.E. and Blanchoin, L. (2010) Regulation of actin dynamics by actin-binding proteins in pollen. *J. Exp. Bot.* **61**, 1969–1986.
Su, H., Wang, T., Dong, H. and Ren, H. (2007) The villin/gelsolin/fragmin superfamily proteins in plants. *J. Integr. Plant Biol.* **49**, 1183–1191.
Taylor, N.G., Howells, R.M., Huttly, A.K., Vickers, K. and Turner, S.R. (2003) Interactions among three distinct CesA proteins essential for cellulose synthesis. *Proc. Natl Acad. Sci. USA*, **100**, 1450–1455.
Tominaga, M., Yokota, E., Vidali, L., Sonobe, S., Hepler, P.K. and Shimmen, T. (2000) The role of plant villin in the organization of the actin cytoskeleton, cytoplasmic streaming and the architecture of the transvacuolar strand in root hair cells of *Hydrocharis*. *Planta*, **210**, 836–843.
Turner, S., Gallois, P. and Brown, D. (2007) Tracheary element differentiation. *Annu. Rev. Plant Biol.* **58**, 407–433.
Van der Honing, H., Kieft, H., Emons, A.M. and Ketelaar, T. (2012) *Arabidopsis* VILLIN2 and VILLIN3 are required for the generation of thick actin filament bundles and for directional organ growth. *Plant Physiol.* **158**, 1426–1438.
Vanstraelen, M., Van Damme, D., De Rycke, R., Mylle, E., Inze, D. and Geelen, D. (2006) Cell cycle-dependent targeting of a kinesin at the plasma membrane demarcates the division site in plant cells. *Curr. Biol.* **16**, 308–314.
Walsh, T.P., Weber, A., Higgins, J., Bonder, E.M. and Mooseker, M.S. (1984) Effect of villin on the kinetics of actin polymerization. *Biochemistry*, **23**, 2613–2621.
Wightman, R. and Turner, S.R. (2008) The roles of the cytoskeleton during cellulose deposition at the secondary cell wall. *Plant J.* **54**, 794–805.
Ye, Z.H., Freshour, G., Hahn, M.G., Burk, D.H. and Zhong, R. (2002) Vascular development in *Arabidopsis*. *Int. Rev. Cytol.* **220**, 225–256.
Yokota, E. and Shimmen, T. (1998) Actin-bundling protein isolated from pollen tubes of lily. Biochemical and immunocytochemical characterization. *Plant Physiol.* **116**, 1421–1429.
Yokota, E., Muto, S. and Shimmen, T. (2000) Calcium–calmodulin suppresses the filamentous actin-binding activity of a 135-kilodalton actin-bundling protein isolated from lily pollen tubes. *Plant Physiol.* **123**, 645–654.
Yokota, E., Vidali, L., Tominaga, M., Tahara, H., Orii, H., Morizane, Y., Hepler, P.K. and Shimmen, T. (2003) Plant 115-kDa actin-filament bundling protein, P-115-ABP, is a homologue of plant villin and is widely distributed in cells. *Plant Cell Physiol.* **44**, 1088–1099.
Yokota, E., Tominaga, M., Mabuchi, I., Tsuji, Y., Staiger, C.J., Oiwa, K. and Shimmen, T. (2005) Plant villin, lily P-135-ABP, possesses G-actin binding activity and accelerates the polymerization and depolymerization of actin in a Ca^{2+}-sensitive manner. *Plant Cell Physiol.* **46**, 1690–1703.
Zhang, H., Qu, X., Bao, C., Khurana, P., Xie, Y., Zheng, Y., Chen, N., Blanchoin, L., Staiger, C.J. and Huang, S. (2010) *Arabidopsis* VILLIN5, an actin filament bundling and severing protein, is necessary for normal pollen tube growth. *Plant Cell*, **22**, 2749–2767.
Zhang, Y., Xiao, Y., Du, F., Cao, L., Dong, H. and Ren, H. (2011) *Arabidopsis* VILLIN4 is involved in root hair growth through regulating actin organization in a Ca^{2+}-dependent manner. *New Phytol.* **190**, 667–682.
Zhong, R., Taylor, J.J. and Ye, Z.H. (1997) Disruption of interfascicular fiber differentiation in an *Arabidopsis* mutant. *Plant Cell*, **9**, 2159–2170.

Zhong, R., Burk, D.H., Morrison, W.H. III and Ye, Z.H. (2002) A kinesin-like protein is essential for oriented deposition of cellulose microfibrils and cell wall strength. *Plant Cell*, **14**, 3101–3117.

Zhong, R., Burk, D.H., Morrison, W.H. III and Ye, Z.H. (2004) *FRAGILE FIBER3*, an *Arabidopsis* gene encoding a type II inositol polyphosphate 5-phosphatase, is required for secondary wall synthesis and actin organization in fiber cells. *Plant Cell*, **16**, 3242–3259.

Zhong, R., Burk, D.H., Nairn, C.J., Wood-Jones, A., Morrison, W.H. III and Ye, Z.H. (2005a) Mutation of SAC1, an Arabidopsis SAC domain phosphoinositide phosphatase, causes alterations in cell morphogenesis, cell wall synthesis, and actin organization. *Plant Cell*, **17**, 1449–1466.

Zhong, R., Pena, M.J., Zhou, G.K., Nairn, C.J., Wood-Jones, A., Richardson, E.A., Morrison, W.H. III, Darvill, A.G., York, W.S. and Ye, Z.H. (2005b) *Arabidopsis Fragile Fiber8*, which encodes a putative glucuronyltransferase, is essential for normal secondary wall synthesis. *Plant Cell*, **17**, 3390–3408.

Zhong, R., Demura, T. and Ye, Z.H. (2006) SND1, a NAC domain transcription factor, is a key regulator of secondary wall synthesis in fibers of *Arabidopsis*. *Plant Cell*, **18**, 3158–3170.